

Organic & Biomolecular Chemistry

Accepted Manuscript



This is an *Accepted Manuscript*, which has been through the Royal Society of Chemistry peer review process and has been accepted for publication.

Accepted Manuscripts are published online shortly after acceptance, before technical editing, formatting and proof reading. Using this free service, authors can make their results available to the community, in citable form, before we publish the edited article. We will replace this *Accepted Manuscript* with the edited and formatted *Advance Article* as soon as it is available.

You can find more information about *Accepted Manuscripts* in the [Information for Authors](#).

Please note that technical editing may introduce minor changes to the text and/or graphics, which may alter content. The journal's standard [Terms & Conditions](#) and the [Ethical guidelines](#) still apply. In no event shall the Royal Society of Chemistry be held responsible for any errors or omissions in this *Accepted Manuscript* or any consequences arising from the use of any information it contains.

Relative stability of benziporphyrin and naphthiporphyrin tautomers and the emergence of macrocyclic diatropicity

Deyaa I AbuSalim and Timothy D. Lash*

Department of Chemistry, Illinois State University, Normal, Illinois 61790-4160

E-mail: tdlash@ilstu.edu

Abstract

The conformations of a series of benziporphyrins, naphthiporphyrins, oxybenziporphyrins, and related structures were minimized using DFT-B3LYP/6-311++G(d,p). The relative stabilities of the tautomers for each series were calculated using M06-2X and B3LYP-D functionals, and bond lengths were obtained. The diatropic properties of each species were assessed by calculating nucleus independent chemical shifts (NICS) and the related NICS_{zz} values. Although benziporphyrin and naphthiporphyrin tautomers essentially exhibit no aromatic properties, mono- and diprotonated species show weakly diatropic characteristics in agreement with experimental observations. Benziphlorins, intermediates in the MacDonald “3 + 1” synthesis of benziporphyrins, were also examined and tautomers with methylene units adjacent to the benzene ring were shown to be far more stable than tautomers with a CH_2 bridge between two pyrrolic units. 2-Hydroxybenziporphyrin was shown to be significantly less stable than the aromatic tautomer oxybenziporphyrin, although diprotonation leads to a species with somewhat reduced diatropicity. Related systems were also analyzed and the results demonstrate that benziporphyrins and naphthiporphyrins range from structures with no measurable macrocyclic aromaticity to strongly aromatic systems that exhibit large diamagnetic ring currents.

Introduction

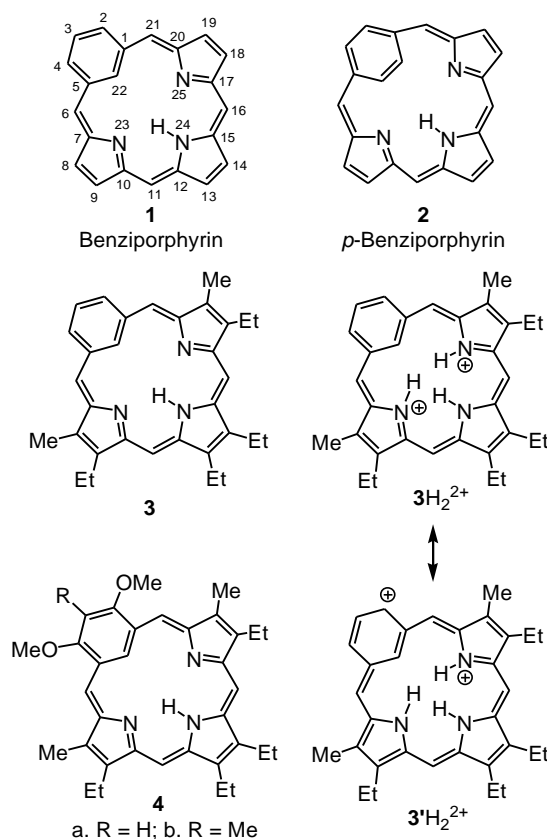
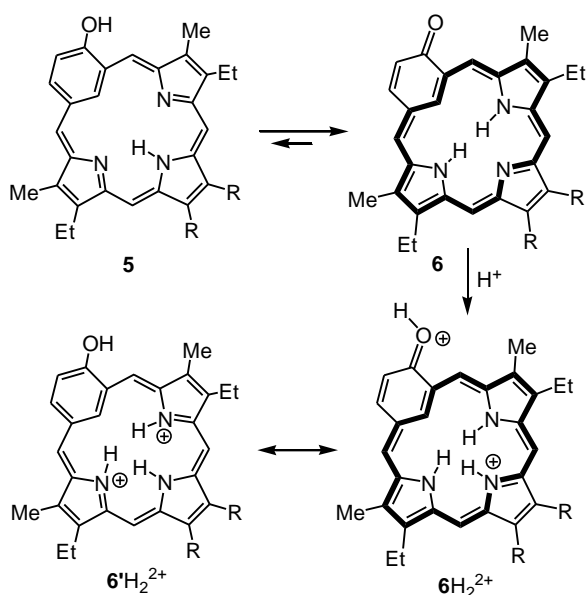


Figure 1. Structures of benziporphyrins.

Benziporphyrins **1** are an important class of porphyrin analogues in which one of the pyrrolic subunits is replaced by a benzene ring.^{1,2} The benzene moiety in regular benziporphyrins is attached in a 1,3-fashion and for this reason they are sometimes referred to as *m*-benziporphyrins.³ *p*-Benziporphyrins **2** have also been prepared,⁴ but will not be discussed in this paper. The feasibility of synthesizing benziporphyrins was first demonstrated in 1994,⁵ and a superior procedure for preparing isomerically pure benziporphyrins was reported shortly thereafter.^{1,6} The proton NMR spectrum for benziporphyrin **3** (Figure 1) gives no indication of a macrocyclic ring current as the internal and external protons on the arene unit show up very close together (7.7-8.0 ppm) in the proton NMR spectrum for this compound.¹ However, in the

presence of trifluoroacetic acid (TFA), a dication 3H_2^{2+} was generated where the internal CH shifted upfield to 5 ppm.^{1,7} This shift has been interpreted as being due to the emergence of a weak diamagnetic ring current arising from resonance contributors such as $3'\text{H}_2^{2+}$ that possess 18π electron delocalization pathways. Dimethoxybenzporphyrins **4** appear to show a weak diatropic ring current even for the free base forms, particularly when $\text{R} = \text{H}$, and this is greatly enhanced in the diprotonated porphyrinoids.⁸ Similar results were obtained for dimethoxytetraarylporphyrins.⁹



Scheme 1. Tautomerization and protonation of oxybenzporphyrins.

When a hydroxy-group is introduced on the 2-position of benzporphyrin (structure **5**), a tautomerization takes place to give a strongly aromatic semiquinone-containing porphyrinoid named oxybenzporphyrin (**6**, Scheme 1).^{1,6,10} In the proton NMR spectrum of **6**, the internal CH proton appeared at -7.2 ppm. Given that the equivalent proton in **3** shows up at 7.8 ppm, this resonance has been shifted upfield by a remarkable 15 ppm due to the simple expedient of introducing a hydroxyl substituent.¹ The NH protons are also highly shielded, appearing at -4

ppm, while the external *meso*-protons are strongly deshielded to between 8.8 and 10.3 ppm. Tetraphenylxybenzporphyrin showed reduced diatropic character compared to **6** due to steric crowding, but otherwise gave similar results.¹¹ Addition of TFA to **6** resulted in the stepwise formation of mono- and diprotonated species.^{1,6} The dication $\mathbf{6H}_2^{2+}$ showed a substantial loss of diatropic properties and this was rationalized as being due to it taking on significant phenolic character from canonical forms such as $\mathbf{6'H}_2^{2+}$. Related naphthiporphyrins **7** and **8** (Figure 2) have also been reported^{7,12} and these show similar properties, although a slight increase in diatropic character was noted for **8** and the diprotonated form of **7** compared to the related benziporphyrins.⁷ Direct routes to *meso*-tetraarylbenzporphyrins **9a** have been developed^{13,14} and the coordination chemistry for these porphyrinoids has been investigated.^{3,15} Even the introduction of an electron-donating *tert*-butyl group in **9b** has been shown to enhance the diatropic characteristics of the diprotonated species.¹⁴ Benziporphyrins have attracted a considerable amount of attention due in part to their ability to form diverse coordination complexes.³ Benziporphyrins also undergo selective oxidative substitution reactions on the internal carbon in the presence of silver(I) salts.^{13,16} Oxybenzporphyrins and related systems have been shown to form stable silver(III) and gold(III) derivatives,^{7,11,12} and *meso*-unsubstituted benziporphyrins and naphthiporphyrins have been reported to form nickel(II) and palladium(II) organometallic derivatives.⁷ In addition, a dihydrobenzporphyrin has shown promise as a fluorescence switch-on sensor for zinc cations,¹⁷ and a related porphyrinoid has been used in the construction of multidimensional nanostructure arrays.¹⁸ Benziporphyrins also provide a valuable probe for porphyrinoid aromaticity due to the wide range of properties exhibited by these systems.^{1,19} In order to gain a better understanding of porphyrinoids based on the benziporphyrin platform, the properties of benziporphyrins have been examined using density functional theory

computations²⁰⁻²³ so that the conformations and relative stabilities of tautomeric species could be assessed. Theoretical studies have shown that the aromatic properties of porphyrinoid systems are due to a superimposition of all possible conjugative pathways, including those due to the individual 6π electron subunits.²⁴⁻³⁰ In this paper, the aromatic characteristics of benziporphyrin structures have been judged using nucleus independent chemical shift calculations (NICS),³¹ and this has allowed an assessment of the emergence of aromaticity due to structural modifications of the benziporphyrin macrocycle.

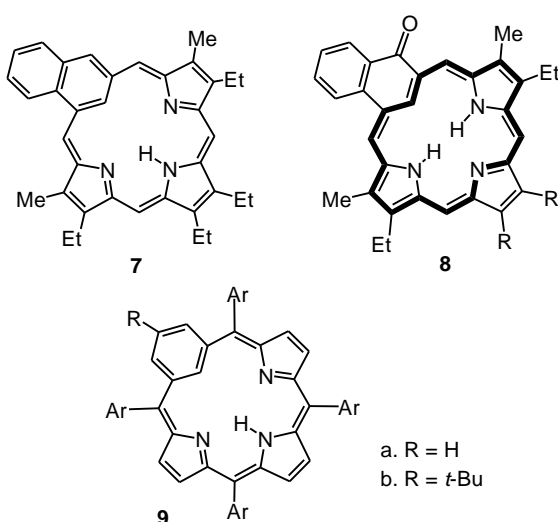


Figure 2. Benzi- and naphthiporphyrins.

Results and Discussion

Benziporphyrin, naphthiporphyrin and heterobenziporphyrins

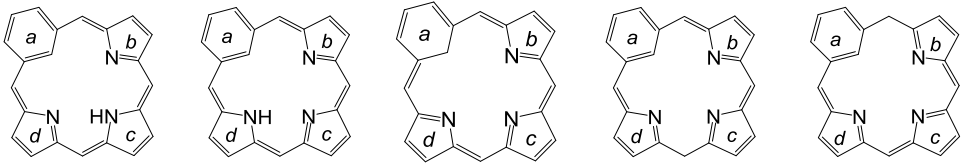
Benzi- and naphthiporphyrin structures were assessed using DFT-B3LYP/6-311++G(d,p). Although B3LYP has been shown to be very good at predicting porphyrinoid geometries and frequencies,^{32,33} the sensitivities of the relative energies to the choice of functionals needed to be assessed.^{34,35} In order to account for this issue, single point energy (SPE) calculations were performed on the minimized structures using M06-2X/6-311++G(d,p) and B3LYP-D/6-

311++G(d,p).^{36,37} The relative energies obtained from the M06-2X and the B3LYP-D functionals were in complete agreement with the trends calculated using the B3LYP functional. In addition, the aromatic character of these molecules was assessed using the GIAO method, which has been consistently used as a reliable probe of porphyrinoid diatropic currents.³⁸⁻⁴⁰ For benziporphyrin, five tautomers were considered (Table 1) which differ by the placement of a single hydrogen. The structures are labeled to indicate the position of this hydrogen, so that the most favored tautomer of benziporphyrin is designated as **BzP-24-H**. This tautomer places the NH opposite to the benzene moiety and this arrangement minimizes steric interactions while introducing favorable hydrogen bonding interactions. Tautomer **BzP-23-H** is calculated to be 7.21-7.91 kcal/mol higher in energy, in part due to increased lone pair-lone pair interactions between the two pyrroline rings. The difference in Gibbs free energy (ΔG) was shown to be 6.95 kcal/mol. Throughout this study, the ΔG and ΔH values showed the same trends, indicating that entropic factors do not play a significant role. Although these tautomers are both nearly planar (Table S1, electronic supplementary material), the bond lengths in **BzP-24-H** (Figure 3) are consistent with a mostly localized π -electron framework.

Nucleus independent chemical shifts (NICS) are used to assess the diatropic character of these species. NICS provide a measure of the upfield and downfield shifts within a structure, and a strongly negative value is correlated to aromatic character.³¹ The standard NICS calculations include the influences of both σ and π -electrons. NICS_{zz} calculations provide an alternative measure that can give valuable insights into the aromatic character.⁴¹ When the measurements are made at reasonably large distances away from the ring center, NICS_{zz} primarily measures the contribution from the π -system.⁴¹⁻⁴⁴ Commonly, the calculations are carried out 1 Å above the ring (NICS(1)_{zz}). The magnitude of the calculated values varies considerably between the two

techniques, and much larger values are obtained with NICZ_{zz} .⁴¹⁻⁴⁴ For instance, we calculated the $\text{NICS}(0)$ value for benzene as -8.16, while $\text{NICS}(1)_{zz}$ gave a value of -28.96. Similarly, nonaromatic cyclopentadiene gave -3.08 for $\text{NICS}(0)$, but -12.22 for $\text{NICS}(1)_{zz}$. Hence, strongly aromatic rings typically give $\text{NICS}(1)_{zz}$ values of >-20 , while -5 may be indicative of significant diatropicity using $\text{NICS}(0)$. Initially our calculations made use of NICS and for the most part these are the results which are discussed as both methods showed the same trends. Nevertheless, $\text{NICS}(1)_{zz}$ values were calculated for each species and these can be considered to be a more rigorous measure of diatropic character. The central positions in macrocycles **BzP-24-H** and **BzP-23-H** gave small $\text{NICS}(0)$ values, indicating that there is no more than a trace amount of overall aromatic character (Table 1). The benzene unit (ring *a*) gave values of -4.36 and -5.28, while pyrrole rings *b* and *c*, respectively, gave values of approximately -4.5 (Table 1). However, the pyrrolenine rings gave very low NICS values. These data show that the individual benzene and pyrrole rings retain some aromatic character, but the pyrrolenine units are essentially nonaromatic. Tautomer **BzP-22-H** has an 18π electron delocalization pathway and this is reflected in the highly diatropic $\text{NICS}(0)$ value of -13.30 (the $\text{NICS}(1)_{zz}$ value is -32.38). Ring *a* gives a NICS value of -16.67 because it lies within the 18π electron circuit, but the pyrrolenine units afford positive values because these rings lie outside of the [18]annulene-like pathway and are therefore deshielded. However, **BzP-22-H** is 42.75-48.01 kcal/mol less stable than its nonaromatic tautomer **BzP-24-H**. The ring is calculated to be planar, but it is destabilized by the presence of three lone pairs of electrons within the macrocyclic cavity, as well as by loss of the thermodynamically favored benzene ring. Two additional tautomers, **BzP-11-H** and **BzP-6-H**, were considered with three pyrrolenine rings and a methylene bridge. These isobenziporphyrins

were also very high in energy and gave negligible NICS(0) values as expected for nonaromatic species (Table 1).



	BzP-24-H	BzP-23-H	BzP-22-H	BzP-11-H	BzP-6-H
Rel. ΔG	0.00	6.95	39.94	34.51	35.82
B3LYP/M06-2X/B3LYP-D	0.00/ 0.00 /0.00	7.21/ 7.91 /7.46	42.75/ 48.01 /42.96	36.45/ 33.21 /37.42	37.66/ 35.90 /38.55
NICS(0)/	-1.03/	-1.20/	-13.30/	+1.44/	+0.16/
NICS(1)zz	-0.95	-1.54	-32.38	+6.30	+3.31
NICS(a)/	-4.36/	-5.28/	-16.67/	-5.01/	-5.82/
NICS(1a)zz	-16.69	-18.12	-49.38	-19.27	-21.31
NICS(b)/	-0.82/	-0.28/	+2.50/	-0.99/	+2.10/
NICS(1b)zz	-7.28	-6.30	-2.06	-7.85	-1.95
NICS(c)/	-4.52/	+0.12/	+3.64/	+1.25/	+0.56/
NICS(1c)zz	-11.62	-5.73	-0.04	-4.06	-5.39
NICS(d)/	-0.82/	-4.48/	+2.50/	-0.18/	-1.31/
NICS(1d)zz	-7.28	-10.61	-2.06	-6.50	-8.68

Table 1. Calculated energies (hartrees), relative energies (kcal/mol), NICS and NICS_{zz} values (ppm) for benziporphyrin tautomers.

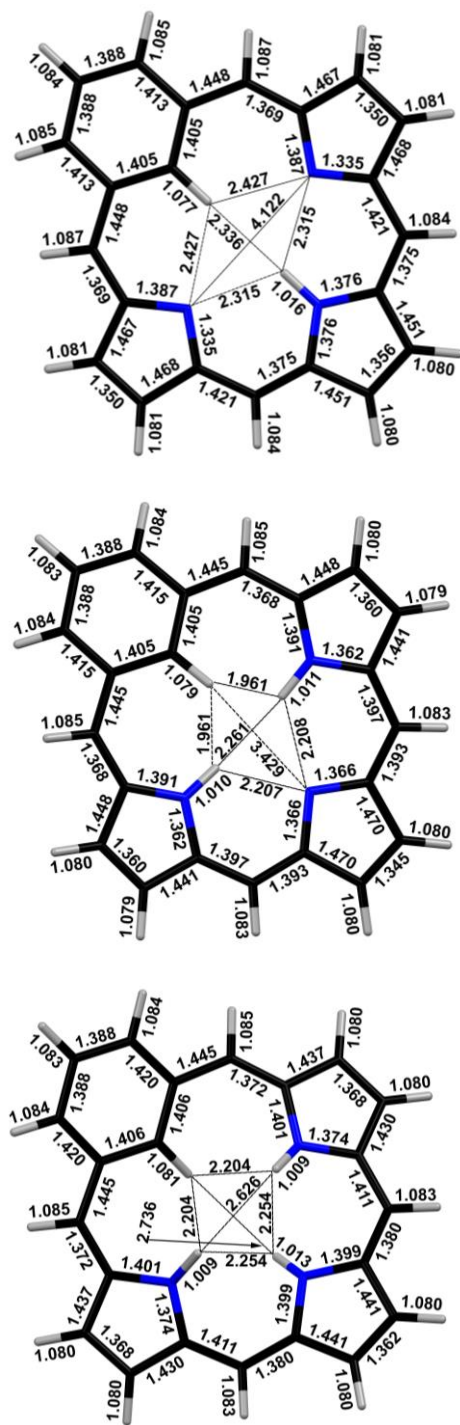
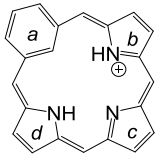
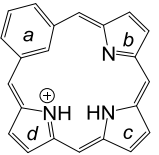
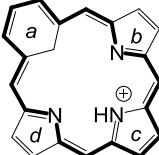
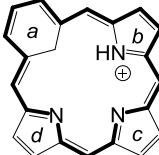


Figure 3. Bond lengths (Å) for selected minimized benziporphyrins: free base **BzP-24-H**, monocation **BzP23,25-H⁺** and dication **BzP-23,24,25-H²⁺**.

				
Rel. ΔG	0.00	3.22	18.98	26.18
B3LYP/M06-2X/B3LYP-D	0.00/0.00/0.00	3.09/2.50/3.07	20.18/23.62/20.09	27.48/31.33/27.63
NICS(0)/	-3.90/	-3.06/	-14.02/	-13.94/
NICS(1)zz	-9.07	-6.49	-34.95	-34.52
NICS(a)/	-5.05/	-3.33/	-17.51/	-17.78/
NICS(1a)zz	-16.07	-12.63	-52.50	-52.25
NICS(b)/	-6.00/	-1.28/	+2.76/	-10.53/
NICS(1b)zz	-14.90	-8.65	-1.39	-28.55
NICS(c)/	+1.60/	-5.62/	-10.07/	+2.86/
NICS(1c)zz	-3.21	-15.67	-28.31	-1.39
NICS(d)/	-6.00/	-6.43/	+2.75/	+4.55/
NICS(1d)zz	-14.90	-13.26	-1.39	+2.51

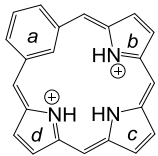
			
Rel. ΔG	0.00	13.43	17.81
B3LYP/M06-2X/B3LYP-D	0.00/0.00/0.00	14.74/19.63/15.23	18.91/24.16/19.52
NICS(0)/	-4.33/	-14.71/	-14.65/
NICS(1)zz	-9.48	-36.16	-36.20
NICS(a)/	-2.29/	-18.76/	-18.13/
NICS(1a)zz	-8.77	-55.14	-54.29
NICS(b)/	-7.61/	-10.26/	+3.31/
NICS(1b)zz	-15.90	-28.23	-0.17
NICS(c)/	-6.31/	+2.70/	-10.40/
NICS(1c)zz	-22.69	-1.88	-28.82
NICS(d)/	-7.61/	-10.26/	-11.43/
NICS(1d)zz	-15.90	-28.23	-30.17

Table 2. Calculated energies (hartrees), relative energies (kcal/mol), NICS and NICS_{zz} values (ppm) for protonated benziporphyrins.

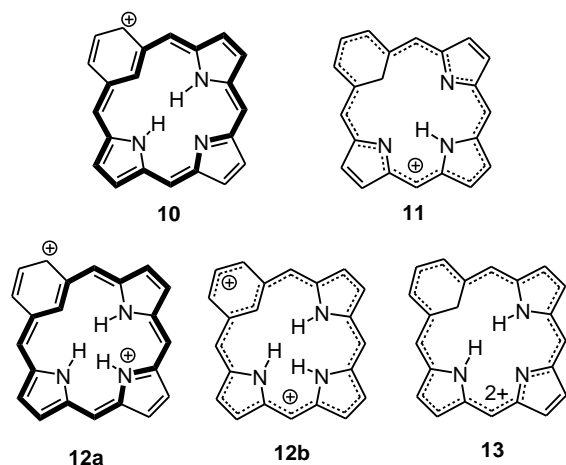


Figure 4. Selected conjugation pathways in protonated benziporphyrins

Although the proton NMR spectrum for benziporphyrin shows no indication of a diamagnetic ring current,¹ addition of TFA generated a dication that exhibited a degree of diatropicity. This phenomenon can also be seen in *meso*-tetraaryl substituted benziporphyrins.⁹ In order to further examine these observations, mono- and diprotonated benziporphyrins were investigated. Four tautomeric forms of monoprotonated benziporphyrin were considered (Table 2). The most stable tautomer, **BzP-23,25-H⁺**, has a NICS(0) value of -3.90, which is consistent with the emergence of a degree of aromatic character. The NICS value for the benzene unit (ring *a*) shows a decreased NICS value presumably due to the arene moiety lying outside of an 18 π electron delocalization pathway. Rings *b* and *d* have strongly negative values, but the pyrrolenine ring *c* gave a low positive value again indicating that this ring lies outside of the 18 π electron circuit. The results are consistent with contributions from canonical forms such as **10** (Figure 4). The calculated bond lengths for **BzP-23,25-H⁺** still show a high degree of bond length alternation, as expected for this weakly diatropic species. Tautomer **BzP-23,24-H⁺** is 2.50-3.09 kcal/mol higher in energy due to reduced opportunities for intramolecular hydrogen bonding, but also gives a weakly aromatic NICS(0) value of -3.06. Tautomer **BzP-22,24-H⁺** shows a strong diatropic ring

current with a NICS value of -14.02, but it is nevertheless 20.09-23.62 kcal/mol less stable than cation **BzP-23,25-H⁺**. Although the presence of an internal CH₂ allows **BzP-22,24-H⁺** to be planar and the NH is ideally placed for hydrogen bonding, the loss of the 6π arene aromaticity decreases the stability of this structure. Nevertheless, this type of tautomer is relatively stable compared to the equivalent free base form **BzP-11-H**. The related tautomer **BzP-22,23-H⁺** is 7.30-7.71 kcal/mole less stable due to steric crowding and reduced hydrogen bonding interactions. In these two tautomers, the six-membered rings (*a*) give strongly negative values, as do the protonated pyrrole rings, but the remaining five-membered rings are deshielded. This indicates that these cations favor nineteen-atom 18π electron delocalization pathways as illustrated for **BzP-22,24-H⁺** with structure **11** (Figure 4). Three diprotonated benziporphyrin dications were also considered (Table 2). The lowest energy tautomer, **BzP-23,24,25-H²⁺**, has four internal hydrogens and the resulting steric crowding causes the ring to be relatively nonplanar (Table S1). Specifically, the benzene ring is tilted 17.54° from the mean macrocyclic plane, and rings *b* and *c* are also tilted by approximately 15°. **BzP-23,24,25-H²⁺** gives a NICS(0) value of -4.33, in line with the observed increase in diatropic character for **3H²⁺** by proton NMR spectroscopy.¹ Although the diatropic character can be ascribed to canonical forms such as **12a**,⁷ the NICS values for the individual rings are more consistent with the presence of a cationic nineteen-atom delocalization pathway such as the one shown in structure **12b** (Figure 4). **BzP-23,24,25-H²⁺** still shows significant bond length alternation, but this is reduced compared to the corresponding free base and monocationic structures (Figure 3). Two higher energy tautomers were considered with internal methylene units. **BzP-22,23,25-H²⁺** and **BzP-22,23,24-H²⁺** are planar (Table 2) and possess aromatic delocalization pathways, but are 14.74-19.63 and 18.91-24.16 kcal/mol higher in energy, respectively, than **BzP-23,24,25-H²⁺**. **BzP-22,23,25-H²⁺** is the

more favored of the two because the NHs have more favorable hydrogen bonding interactions. These tautomers are again far closer in energy to the form with an intact benzene ring than is the case for free base tautomers such as **BzP-22-H** where destabilization is exacerbated due to severe lone pair-lone pair repulsions. Nevertheless, the penalty for losing the aromatic character of the benzene subunit still reduces the overall stability. **BzP-22,23,25-H²⁺** has a NICS(0) value of -14.71 (NICS_{zz} -36.16) and the six-membered ring also exhibits a strongly aromatic value of -18.76. The protonated pyrrole units have NICS values of -10.26, but the remaining ring (c) affords a positive value. These results imply that the system favors a twenty-atom delocalization pathway as illustrated in structure **13** (Figure 4). Similar results were obtained for **BzP-22,23,24-H²⁺**, although it is ring *d* that gives the positive NICS value in this case. The NICS_{zz} results consistently supported these analyses.

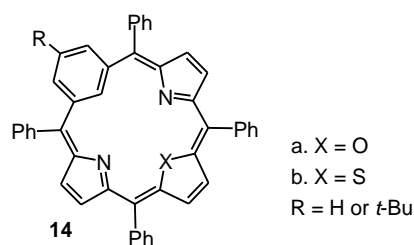
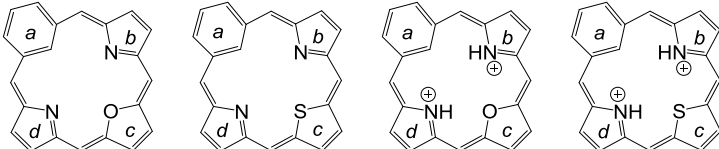


Figure 5. Oxa- and thiabenziporphyrins.

Examples of tetraphenyl oxa- and thiabenziporphyrins **14** were reported recently⁴⁵ and these hetero-analogues also showed a degree of aromatic character for the protonated structures (Figure 5). 24-Oxa-benziporphyrin **24-O-BzP** was examined and the NICS calculations showed no indication of a macrocyclic ring current (Table 3). The benzene and furan rings showed a degree of aromatic character for the individual rings, but the pyrroline rings gave negligible NICS values. Similar results were obtained for the thiophene analogue **24-S-BzP**. Both of the heterobenziporphyrins are planar and the bond lengths are consistent with the presence of

localized π -systems (Figure 6). Addition of acid gave the corresponding dication and the calculated NICS(0) values for these species (**24-O-BzPH₂²⁺** and **24-S-BzPH₂²⁺**, respectively) were close to -5, which is consistent with the presence of a weak diamagnetic ring current (Table 3).



	24-O-BzP	24-S-BzP	24-O-BzPH₂²⁺	24-S-BzPH₂²⁺
NICS(0)/	-0.70/	-1.99/	-4.56/	-5.19/
NICS(1)zz	-0.06	-2.09	-10.72	-10.01
NICS(a)/	-3.72/	-4.70/	-2.14/	-2.22/
NICS(1a)zz	-15.50	-17.81	-8.93	-8.93
NICS(b)/	-0.60/	-0.72/	-7.48/	-7.73/
NICS(1b)zz	-7.04	-6.99	-17.24	-22.77
NICS(c)/	-5.46/	-4.48/	-8.67/	-8.87/
NICS(1c)zz	-13.85	-8.84	-22.83	-11.94
NICS(d)/	-0.60/	-0.72/	-7.48/	-7.73/
NICS(1d)zz	-7.04	-6.99	-17.24	-22.77

Table 3. Calculated energies (hartrees) and NICS values (ppm) for heterobenzporphyrins.

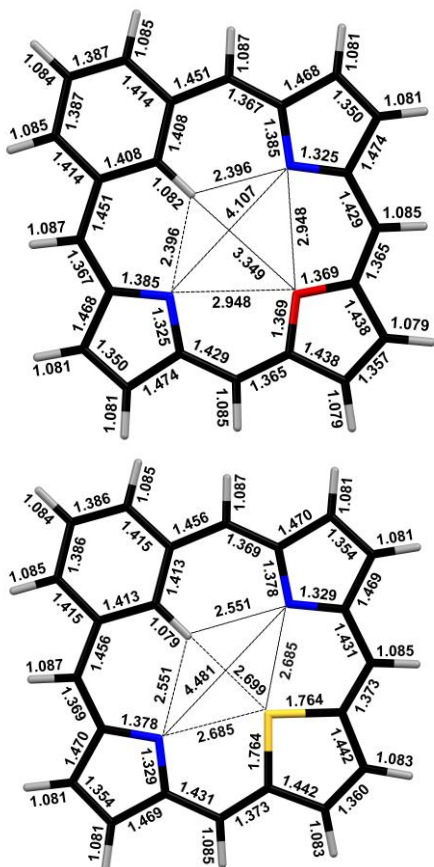
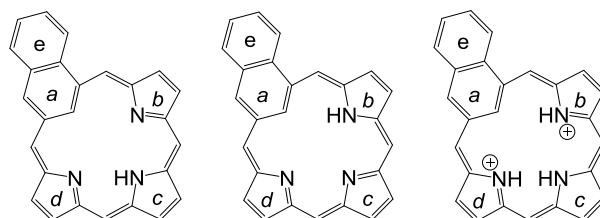


Figure 6. Bond lengths (Å) for minimized heterobenziporphyrins **24-O-BzP** and **24-S-BzP**.



	NP-24-H	NP-23-H	NPH ₂ ²⁺
Rel. ΔG	0.00	6.54	*****
B3LYP/M06-2X/B3LYP-D	0.00/0.00/0.00	7.15/7.75/7.36	*****
NICS(0)/	-0.93/	-1.05/	-6.69/
NICS(1)zz	-0.42	-0.95	-14.86
NICS(a)/	-4.67/	-4.81/	+0.40/
NICS(1a)zz	-15.36	-16.20	-1.23
NICS(b)/	-0.92/	-4.59/	-8.96/
NICS(1b)zz	-7.58	-10.98	-16.52
NICS(c)/	-4.75/	-0.01/	-7.96/
NICS(1c)zz	-11.89	-6.13	-29.57
NICS(d)/	-1.05/	-0.53/	-9.28/
NICS(1d)zz	-7.58	-6.63	-19.45
NICS(e)/	-6.87/	-6.87/	-5.03/
NICS(1e)zz	-24.11	-24.48	-21.31

Table 4. Calculated energies (hartrees), relative energies (kcal/mol), NICS and NICS_{zz} values (ppm) for naphthiporphyrins.

In some respects there is a competition between benzene and porphyrinoid aromaticity in these structures. Certainly, the more aromatic character that is associated with the cross-conjugated arene unit, the less overall aromaticity will be present in the macrocycle. It was hypothesized that a naphthalene ring would be more likely to give up aromatic character due to the reduced resonance delocalization associated with the individual six-membered rings, and that this might lead to increased porphyrinoid aromaticity.⁷ However, naphthiporphyrin **7** showed no sign of a diatropic ring current by proton NMR spectroscopy. Addition of TFA to the NMR solution led to the formation of a dication that showed slightly increased aromaticity compared to the dication derived from benziporphyrin **3**.⁷ Two tautomers of naphthiporphyrin were considered. Tautomer **NP-24-H** was favored over **NP-23-H** by 7.15-7.75 kcal/mol (Table 4) due in part to optimal hydrogen bonding interactions. In addition, the adjacent lone pair electrons in **NP-23-H** and increased crowding between the interior CH and NH also reduced the stability of this species. Both tautomers are planar (Table S1). The bond lengths calculated for **NP-24-H** were consistent with a localized π -electron structure (Figure 7). The corresponding dication **NPH₂²⁺** gave a NICS(0) value of -6.69, confirming that this species is more aromatic than the dication derived from benziporphyrin (**BzP-23,24,25-H²⁺**). The three pyrrole rings give strongly aromatic NICS values, but ring *a* gives a NICS value of +0.40. The aromatic character of this species was previously explained as being due to contributions by canonical forms such as **15a**, but these data suggest that the aromatic contributors have a nineteen-atom delocalization pathway like the one shown in structure **15b** (Figure 8).

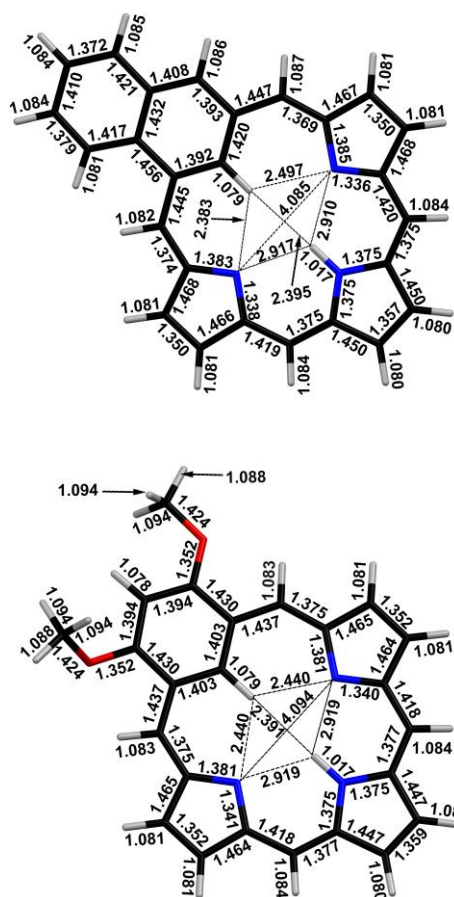


Figure 7. Bond lengths (Å) for minimized naphthiporphyrin **NP-24-H** and dimethoxybenzporphyrin **DiOMeBzP-24-H**.

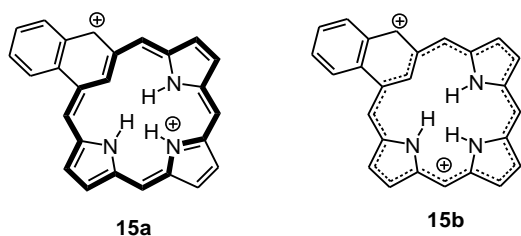
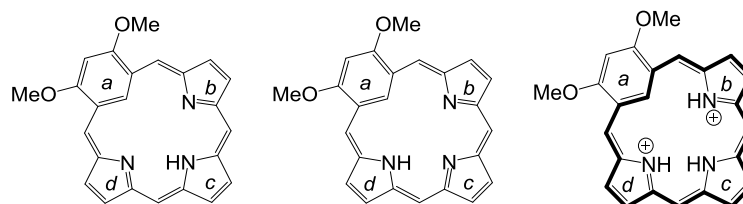


Figure 8. Proposed conjugation pathways in protonated naphthiporphyrin.

Benziporphyrins **4** with methoxy groups on the 2- and 4-positions have been reported, and these show some indication of diatropic character even in the free base forms.^{8,9} The proton

NMR spectrum for benziporphyrin **4a** gave a resonance at 5.07 ppm for the internal CH, which is 2.7 ppm upfield from the resonance observed in benziporphyrin **3**, while the *meso*-protons were shifted downfield to give two 2H singlets at 7.16 and 8.47 ppm.⁸ The effects of the methoxy groups were substantially reduced in **4b** due to steric crowding which inhibits conjugative interactions with the methoxy units.⁸ Two tautomers were considered for 2,4-dimethoxybenzporphyrin. **DiOMe-BzP-24-H** is favored (Table 5) due to the NH being placed in a position that maximizes hydrogen bonding interactions and minimizes steric crowding and lone pair-lone pair repulsion compared to **DiOMe-BzP-23-H**. Both tautomers show moderate NICS(0) values close to -4 which confirm that these are weakly diatropic species (Table 5). The benzene rings in these structures gave very low NICS values, suggesting that these units lie outside of the macrocyclic delocalization pathway. In addition, the pyrroline rings gave low values, but the pyrrole ring produced strongly negative values. The diatropicity of **DiOMe-BzP-24-H** was previously rationalized as being due to resonance contributors such as **16a** (Figure 9) that possess 18 π electron delocalization pathways.⁸ However, the data presented in Table 5 is more consistent with the presence of a seventeen-atom 18 π electron delocalization pathway of the type shown in structure **16b**. The relatively long 7,8-, 9,10-, 17,18- and 19,20-carbon-carbon bonds for **DiOMe-BzP-24-H** (Figure 7) are also consistent with this model. The corresponding dication **DiOMe-BzPH₂²⁺** gave a greatly increased NICS(0) value of -9.81, even though the macrocycle is somewhat distorted due to steric crowding in the internal cavity. The three pyrrole rings all give strongly diatropic NICS values, but surprisingly the benzene ring affords a deshielded value of +4.13 (NICS_{zz} +8.19, Table 5). This indicates that much of the aromatic character for the arene unit has been lost. The aromatic character of **DiOMe-BzPH₂²⁺** has previously been attributed to resonance contributors such as **17a**,⁸ but the data obtained in this

study indicate that it is better described by the nineteen-atom delocalization pathway shown in structure **17b** (Figure 10).



	DiOMe-BzP-24-H	DiOMe-BzP-23-H	DiOMe-BzPH ₂ ²⁺
Rel. ΔG	0.00	7.02	*****
B3LYP/M06-2X/B3LYP-D	0.00/0.00/0.00	7.30/8.04/7.56	*****
NICS(0)/	-3.99/	-4.21/	-9.81/
NICS(1)zz	-8.65	-9.41	-23.17
NICS(a)/	-1.06/	-1.61/	+4.13/
NICS(1a)zz	-2.28	-3.56	+8.19
NICS(b)/	-2.80/	-1.20/	-11.44/
NICS(1b)zz	-10.00	-8.81	-22.04
NICS(c)/	-6.21/	-0.22/	-10.28/
NICS(1c)zz	-15.54	-7.10	-35.63
NICS(d)/	-1.86/	-6.33/	-11.44/
NICS(1d)zz	-9.99	-15.67	-22.00

Table 5. Calculated energies (hartrees), relative energies (kcal/mol), NICS and NICS_{zz} values (ppm) for dimethoxybenzoporphyryns.

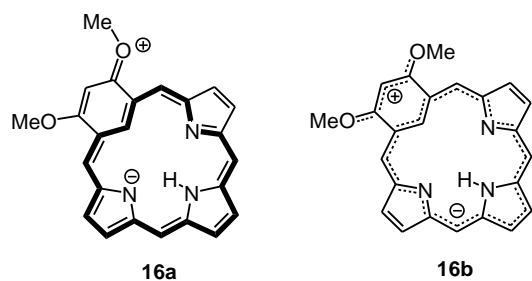


Figure 9. Proposed conjugation pathways in 2,4-dimethoxybenzoporphyryrin.

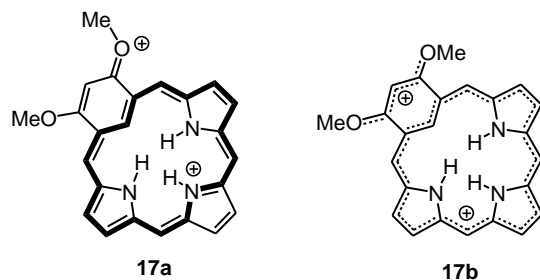
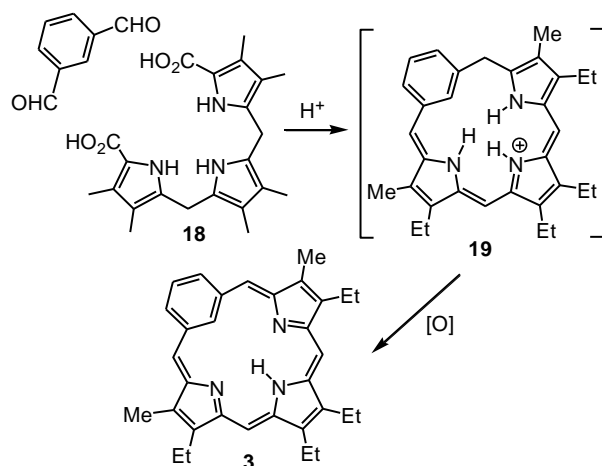


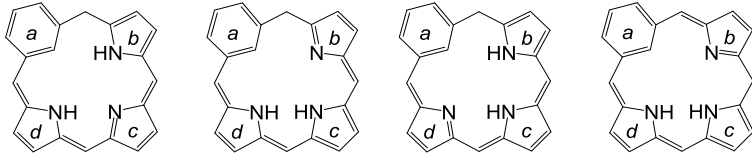
Figure 10. Conjugation pathways in protonated 2,4-dimethoxybenzoporphyryrin.

Benziphlorins

Scheme 2. “3 + 1” Synthesis of benziporphyrin.

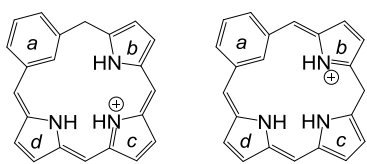
Benziporphyrin **3** was synthesized by an acid catalyzed “3 + 1” condensation⁴⁶ between isophthalaldehyde and a tripyrrane **18** (Scheme 2). A dihydroporphyrinoid or phlorin type intermediate is initially generated,⁴⁶ and subsequent oxidation affords the fully conjugated benziporphyrin. The precise identity of the phlorin intermediate has not been determined. In order to gain insights into the relative stabilities of benziphlorins, four tautomeric species were considered (Table 6). All of these structures are highly distorted and NICS calculations show the expected absence of diatropic character. The pyrrole and benzene rings exhibited NICS values consistent with aromatic 6π electron subunits, but the values were somewhat lower for the pyrroline rings. Pyrrole units with two exocyclic double bonds also showed reduced aromatic character. Interestingly, benziphlorins that have a methylene bridge next to the benzene are far more stable than tautomer **10-BPhl-24,25-H** that has the CH_2 between two pyrrole units. The lowest energy tautomer **5-BPhl-23,25-H** offers the best opportunities for intramolecular hydrogen bonding. In the “3 + 1” synthesis of benziporphyrin (Scheme 2), the phlorin is almost certainly formed as a protonated species. Therefore, the relative energies of protonated

benziphlorins **5-BPhIH⁺** and **10-BPhIH⁺** were calculated (Table 7). Protonation further increased the difference in energy between the two structures, and **5-BPhIH⁺** as shown to be 18.74-19.29 kcal/mol more stable than **10-BPhIH⁺**. In **5-BPhIH⁺**, all of the subunits show reasonably large negative NICS values, although there is no overall diatropic character. In **10-BPhIH⁺**, the aromatic character of the benzene ring is reduced, as is the case for rings *b* and *d* compared to their counterparts in the isomeric structure. However, ring *c* gives a larger NICS value. Both cations are nonplanar, but in **5-BPhIH⁺** by far the largest deviation (46.95°) from the mean macrocyclic plane is for the benzene ring. In **10-BPhIH⁺**, a pyrrole unit is rotated by 46.25° instead. As beneficial conjugation and charge delocalization primarily occurs between the pyrrolic units, the latter conformation is poorly suited to stabilize the structure. These results firmly point toward structure **19** being the intermediate in the synthesis of benziporphyrin **3** (Scheme 2). This is also consistent with the structure of a pyriphlorin that was isolated from a reaction of tripyrrane **18** with 2,6-pyridinedicarbaldehyde in a failed attempt to synthesize a pyriporphyrin.^{47,48}



	5-BPhl-23,25-H	5-BPhl-24,25-H	5-BPhl-23,24-H	10-BPhl-24,25-H
<i>Rel. ΔG</i>	0.00	3.86	5.34	14.44
<i>B3LYP/M06-2X/B3LYP-D</i>	0.00/ 0.00 /0.00	2.29/ 4.50 /4.25	3.82/ 5.89 /5.77	13.55/ 14.45 /15.93
NICS(0)/	-0.38/	-0.31/	+0.06/	+2.32/
NICS(1)zz	+1.22	+2.14	+1.83	+9.67
NICS(<i>a</i>)/	-8.46/	-8.07/	-8.40/	-5.49/
NICS(1<i>a</i>)zz	-25.81	-25.27	-25.21	-19.12
NICS(<i>b</i>)/	-11.22/	-1.13/	-11.93/	-1.13/
NICS(1<i>b</i>)zz	-25.81	-15.00	-27.18	-8.56
NICS(<i>c</i>)/	-3.21/	-10.90/	-5.36/	-10.90/
NICS(1<i>c</i>)zz	-25.23	-22.37	-12.95	-24.15
NICS(<i>d</i>)/	-4.44/	-3.40/	-1.23/	-3.40/
NICS(1<i>d</i>)zz	-10.28	-9.87	-9.19	-6.00

Table 6. Calculated energies (hartrees), relative energies (kcal/mol) and NICS values (ppm) for benziphlorin tautomer.



	5-BPhIH ⁺	10-BPhIH ⁺
<i>Rel. ΔG</i>	0.00	18.15
<i>B3LYP/M06-2X/B3LYP-D</i>	0.00/ 0.00 /0.00	18.74/ 18.77 /19.29
NICS(0)/	-0.34/	+0.04/
NICS(1)zz	+2.91	+3.48
NICS(<i>a</i>)/	-7.83/	-5.19/
NICS(1<i>a</i>)zz	-26.40	-17.78
NICS(<i>b</i>)/	-9.29/	-6.30/
NICS(1<i>b</i>)zz	-20.55	-15.38
NICS(<i>c</i>)/	-6.64/	-10.77/
NICS(1<i>c</i>)zz	-19.55	-32.92
NICS(<i>d</i>)/	-4.63/	-3.82/
NICS(1<i>d</i>)zz	-10.18	-8.30

Table 7. Calculated energies (hartrees), relative energies (kcal/mol), NICS and NICS_{zz} values (ppm) for protonated benzophlorins.

Oxybenzoporphyrin, oxynaphthoporphyrin and a further oxidized system

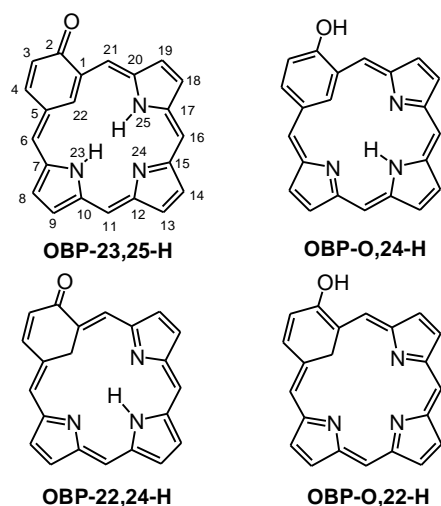


Figure 11. Selected tautomers of oxybenzoporphyrin.

The introduction of a hydroxyl substituent at the 2-position of benziporphyrin (**5**) facilitates a tautomerization to form an aromatic semiquinone-containing porphyrinoid **6** named oxybenzporphyrin (Scheme 1).⁶ The thermodynamic favorability of **6** was attributed to the introduction of a carbonyl moiety together with a porphyrin-like 18 π electron delocalization pathway.⁶ Nevertheless, this occurs at the expense of losing the 6 π -electron arene character of the six-membered ring. Addition of TFA to solutions of **6** initially resulted in the formation of a monocation **6H**⁺ that appeared to retain strongly diatropic characteristics. However, further addition of TFA led to a drastic reduction in the diatropic ring current. The resulting dication **6H**₂²⁺ showed the inner CH at 1.05 ppm, a downfield shift of over 8 ppm compared to **6**, and the *meso*-protons were observed as four 1H singlets at 8.05, 8.10, 8.80 and 9.41.^{1,6} Clearly the dication retains a degree of diatropic character but this is greatly diminished due to phenolic resonance contributors such as **6'**H₂²⁺ (Scheme 1). The UV-vis spectra for free base **6** and



	OBP-23,25-H	OBP-24,25-H	OBP-23,24-H	OBP-O,24-H	OBP-O,23-H
Rel. ΔG	0.00	4.47	5.29	12.45	19.61
B3LYP/M06-2X/B3LYP-D	0.00/0.00/0.00	4.13/3.99/4.06	5.04/4.92/4.98	12.49/8.13/13.41	19.90/16.41/21.08
NICS(0)/	-13.07/	-12.52/	-12.63/	-2.48/	-2.76/
NICS(1)zz	-32.75	-31.47	-31.98	-4.75	-5.53
NICS(a)/	+9.75/	+10.51/	+10.39/	-3.29/	-4.09/
NICS(1a)zz	+18.15	+15.82	+18.95	-9.40	-11.07
NICS(b)/	-12.42/	-13.63/	-3.59/	-1.04/	-0.35/
NICS(1b)zz	-32.17	-28.80	-15.63	-8.14	-6.87
NICS(c)/	-3.22/	-12.55/	-11.98/	-5.39/	+0.05/
NICS(1c)zz	-14.08	-33.50	-28.30	-13.54	-6.14
NICS(d)/	-13.35/	-4.48/	-14.51/	-1.52/	-5.49/
NICS(1d)zz	-33.72	-17.07	-39.93	-8.82	-13.24

Table 8. Calculated energies (hartrees), relative energies (kcal/mol), NICS and NICS_{zz} values (ppm) for tautomers of oxybenzporphyrin.

monocation 6H^+ both gave intense porphyrin-like Soret bands at 428 nm together with a series of Q bands at longer wavelengths.^{1,6} However, dication 6H_2^{2+} gave rise to a spectrum with a weakened Soret band at 434 nm together with broad absorptions in the visible region that were consistent with reduced porphyrinoid aromaticity.^{1,6} Some DFT calculations were previously performed for oxybenzporphyrin and these showed that **OBP-23,25-H** is 12.74 kcal/mol more stable than the phenolic tautomer **OBP-O,24-H** (Figure 11).^{49,50} The numbers used in the structure labels designate the positions of the two mobile protons, and when a hydrogen is attached to the oxygen this is assigned as O. Two less stable tautomers with internal methylene units, **OBP-22,24-H** and **OBP-O,22-H**, were also considered.⁴⁵ Keto structure **OBP-22,24-H** was shown to be 18.07 kcal/mol higher in energy than the most stable tautomer, while the hydroxy tautomer **OBP-O,22-H** is more than 50 kcal/mol higher in energy.⁴⁵ **OBP-22,24-H** is sufficiently low in energy to be reasonably accessible, and was of interest because related palladium(II) 22-alkyl substituted complexes had been isolated.⁴⁵ In this study, we were interested in comparing the stability of lower energy tautomers for the free base, monoprotinated and diprotinated forms of oxybenzporphyrin. The free base calculations were in good agreement with the earlier study.⁴⁹ Three semiquinone tautomers can be identified with **OBP-23,25-H** being lowest in energy (Table 8). **OBP-23,24-H** and **OBP-24,25-H** are 4.92-5.04 and 3.99-4.13 kcal/mol higher in energy due to less favorable hydrogen bonding interactions. In all three cases, three hydrogens are present within the porphyrinoid cavity. The phenolic tautomers **OBP-O,24-H** and **OBP-O,23-H** were calculated to be 8.13-13.41 and 16.41-21.08 kcal/mol, respectively, and the higher value of the latter species is due to a combination of poor hydrogen bonding interactions, increased lone pair-lone pair repulsion and a degree of crowding due to the proximate inner hydrogens. It was also noted that the hydroxy tautomers gave two minima

corresponding to conformers that differed by the orientation of the hydroxyl groups. In order for the oxygen to electronically interact with the system it has to take on sp^2 character, and this means that the OH bond must lie in the plane of the benzene ring. For **OBP-O,24-H**, the more favored conformation orientates the OH to the left away from the macrocycle (designated **OBP-O,24-H-L**) and the alternative conformer **OBP-O,24-H-R** was found to be 1.12 kcal/mol higher in energy (Table 9 and Figure 12). Similarly, **OBP-O,23-H-L** is 0.97 kcal/mol lower in energy than **OBP-O,23-H-R** (Table 9). The bond lengths for **OBP-23,25-H** (Figure 13) were consistent with the [18]annulene model for porphyrinoid aromaticity, as illustrated by structure **20A** (Figure 14), and as expected the 12,13- and 14,15-carbon-carbon bonds are longer than the 7,8-, 9,10-, 17,18- and 19,20-bonds denoting a larger degree of single bond character. NICS calculations for **OBP-23,25-H** gave a NICS(0) value of -13.07 (Table 8), confirming the highly diatropic character of oxybenzporphyrin. Nevertheless, this value is lower than is obtained for porphyrin or carbaporphyrins,⁵¹ possibly due to minor dipolar resonance contributors such as **20B** which could disrupt this pathway (Figure 14). The results are also consistent with the proton NMR data for **6**, as the *meso*-protons are not shifted as far downfield as those for porphyrins and carbaporphyrins. The NICS values for the individual rings were also insightful. Pyrrole rings *b* and *d* lie within the predicted 18π electron pathway and hence show large negative values, although the 6π electron units also contribute to this result. The pyrrolenine ring (*c*) gives a low value because it lies outside of the [18]annulene pathway, while the six-membered ring gives a strongly positive value. These data suggest that the semiquinone unit is strongly deshielded by falling outside of the aromatic delocalization pathway but the effect is much reduced for ring *c* possibly due to minor resonance contributors such as **20C** (Figure 14) that introduce alternative delocalization pathways. The major oxybenzporphyrin tautomer **OBP-23,25-H** is reasonably

flat with ring *a* tilted relative to the mean macrocyclic plane by 3.82° , although **OBP-23,24-H** and **OBP-24,25-H** are slightly more distorted (Table S1). Hydroxybenzporphyrins **OBP-O,24-H** and **OBP-O,23-H** are virtually planar because only two hydrogens remain within the cavity. The NICS(0) value for **OBP-O,24-H** is -2.48, suggesting the presence of a very weak diatropic ring current. This may be due to dipolar resonance contributors such as **20D** that possess 18π electron delocalization pathways (Figure 14). Similar deductions can be made for tautomer **OBP-O,23-H**. In both structures, the pyrrololeone rings give negligible NICS values, and the benzene units also give relatively low values suggesting reduced aromatic character.

OBP-O,24-H-L	OBP-O,24-H-R	OBP-O,23-H-L	OBP-O,23-H-R
-1087.080498	-1087.078708	-1087.068692	-1087.067147
0.00	1.12	0.00	0.97

Table 9. Calculated energies (hartrees) and relative energies (kcal/mol) for hydroxybenzporphyrin conformers.

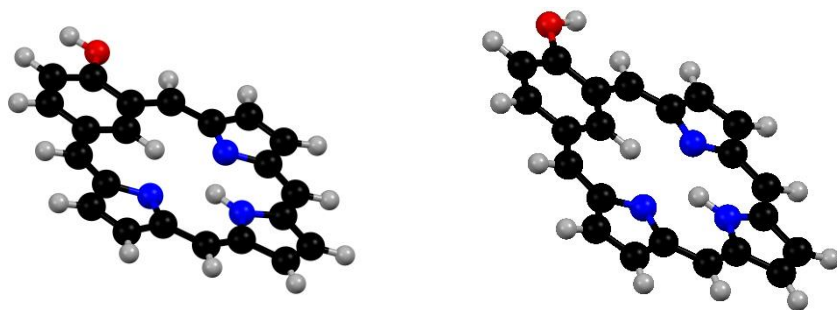


Figure 12. Conformational minima for **OBP-O,24-H** showing the left hand orientation of the OH towards the benzene ring (**OBP-O,24-H-L**) and the right hand version **OBP-O,24-H-R** where the hydroxyl group is pointed towards the *meso*-position.

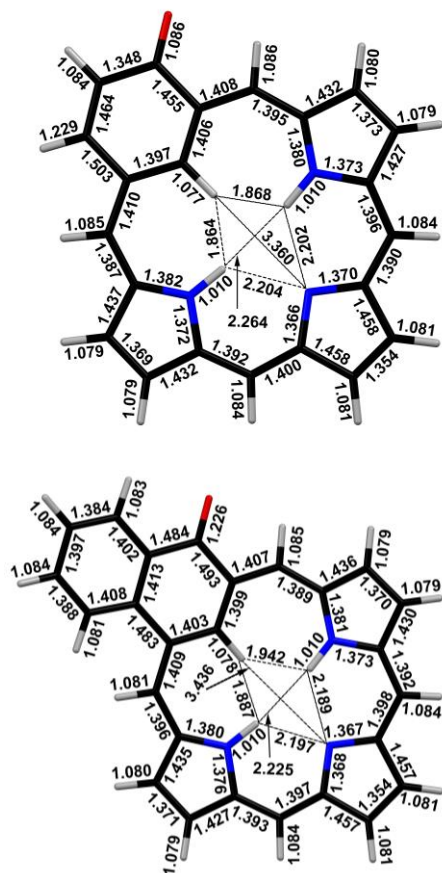


Figure 13. Bond lengths (Å) for oxybenziporphyrin **OBP-23,25-H** and oxynaphthiporphyrin **ONP-23,25-H**.

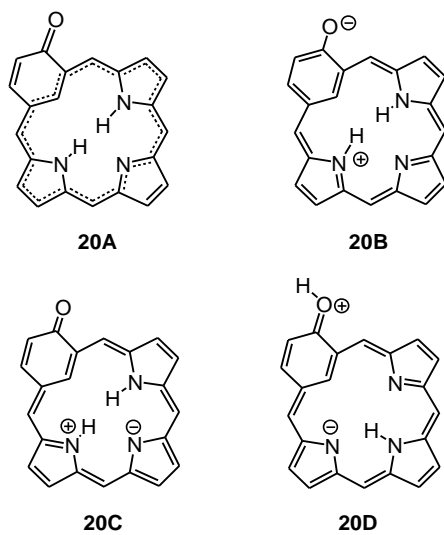
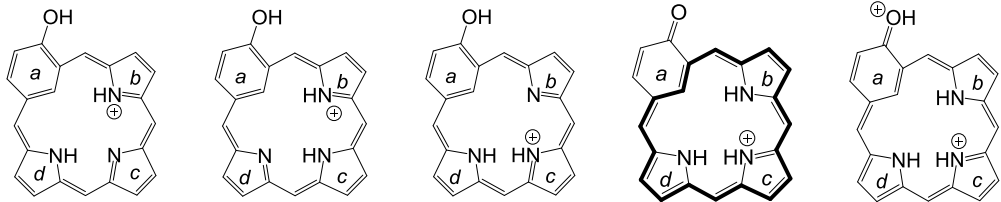


Figure 14. Selected conjugation pathways in oxybenziporphyrins.



	OBP-O,23,25-H⁺	OBP-O,24,25-H⁺	OBP-O,23,24-H⁺	OBP-23,24,25-H⁺	OBPH₂²⁺
Rel. ΔG	0.00	3.03	3.19	5.27	*****
B3LYP/M06-2X/B3LYP-D	0.00/0.00/0.00	2.86/2.43/2.82	3.09/2.69/3.05	5.10/6.96/3.72	*****
NICS(0)/	-6.13/	-5.10/	-5.28/	-13.12/	-7.18/
NICS(1)zz	-14.79	-11.66	-11.57	-32.92	-16.58
NICS(a)/	-2.82/	-1.23/	-1.28/	+11.13/	+0.46/
NICS(1a)zz	-8.23	-2.77	-4.75	+24.46	-1.34
NICS(b)/	-7.21/	-7.65/	-1.57/	-13.69/	-9.06/
NICS(1b)zz	-17.18	-22.28	-9.50	-42.18	-18.06
NICS(c)/	+0.97/	-6.90/	-6.71/	-13.85/	-8.06/
NICS(1c)zz	-4.90	-15.94	-18.86	-26.67	-7.38
NICS(d)/	-7.40/	-1.90/	-7.91/	-14.37/	-9.51/
NICS(1d)zz	-18.43	-10.18	-16.74	-33.68	-19.68

Table 10. Calculated energies (hartrees), relative energies (kcal/mol), NICS and NICS_{zz} values (ppm) for protonated oxybenzporphyrins.

Four monoprotonated oxybenzporphyrin tautomers were considered (Table 10). Unexpectedly, hydroxybenzporphyrin monocation **OBP-O,23,25-H⁺** was the most stable form rather than the oxybenzporphyrin tautomer **OBP-23,24,25-H⁺**. In fact, all three hydroxy-tautomers were favored over the more aromatic keto-tautomer, although the differences in energy were relatively small. As the keto form is apparently generated in the monoprotonation of oxybenzporphyrin **6**,¹ the preferences are presumably affected by solvent interactions. **OBP-23,24,25-H⁺** is the least planar of the series due to the presence of four internal hydrogen atoms (Table S1). **OBP-O,23,25-H⁺** has an optimal arrangement for hydrogen bonding interactions compared to the other hydroxy forms. Each hydroxy tautomer has two conformational minima depending on the orientation of the OH units (Table 11). The differences in energies for these forms range from 2.78-3.44 kcal/mol, which were comparable to the differences in energies for the individual tautomers. In each case, the conformations with the OH orientated to the left away

from the macrocycle were favored. Keto-tautomer **OBP-23,24,25-H⁺** gave a strongly aromatic NICS(0) value of -13.12 (NICS(1)_{zz} -32.92). All three of the five-membered rings also gave strongly negative values but the six-membered ring gave a strongly deshielded value of +11.13. These results are consistent with the presence of a 19-atom delocalization pathway of the type illustrated in structure **21A** (Figure 15). **OBP-O,23,25-H⁺** gave a small but significant NICS(0) value of -6.13 (Table 10). Rings *b* and *d* gave NICS values of -7.21 and -7.40, respectively, but pyrroline ring *c* afforded a very small value and the six-membered ring also gave a low result. This can be interpreted to mean that canonical forms such as **21B** are involved that introduce an eighteen-atom 18 π electron delocalization pathway. Tautomers **OBP-O,23,24-H⁺** and **OBP-O,24,25-H⁺** gave similar results (Table 10) and related delocalization pathways can be proposed. Dication **OBPH₂²⁺** gave a NICS(0) value of -7.18 (Table 10). The structure is moderately nonplanar due to the presence of four hydrogens within the cavity. The reduced aromaticity of **OBPH₂²⁺** compared to the free base form is due to phenolic canonical forms such as **22A** (Figure 15) that interrupt the conjugation pathway. Nevertheless, the NICS values for the individual pyrrole rings are all large, while the six-membered ring gives a small positive value (Table 10), and this suggests the presence of the nineteen-atom delocalization pathway shown in structure **22B** (Figure 10). Dication **OBP-O,23,25-H⁺** also showed two conformational minima (Table 12). Once again the conformer that orientates the OH away from the macrocycle is preferred, but in this case the difference in energy is larger (5.31 kcal/mol).

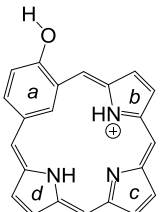
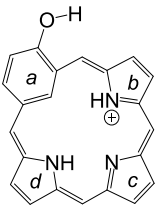
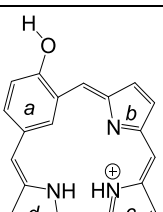
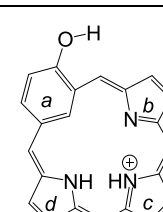
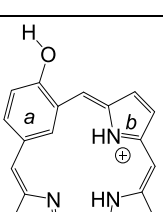
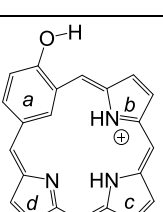
	
OBP-O,23,25-H-L -1087.492664 0.00	OBP-O,23,25-H-R -1087.487586 3.19
	
OBP-O,23,24-H-L -1087.487747 0.00	OBP-O,23,24-H-R -1087.483317 2.78
	
OBP-O,24,25-H-L -1087.48811 0.00	OBP-O,24,25-H-R -1087.482622 3.44

Table 11. Calculated energies (hartrees) and relative energies (kcal/mol) for protonated hydroxybenziporphyrin conformers.

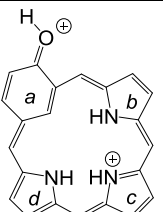
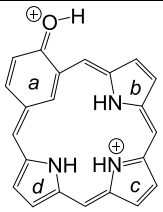
	
OBPH₂²⁺-L -1087.768659 0.00	OBPH₂²⁺-R -1087.760203 5.31

Table 12. Calculated energies (hartrees) and relative energies (kcal/mol) for conformers of diprotonated oxybenziporphyrin.

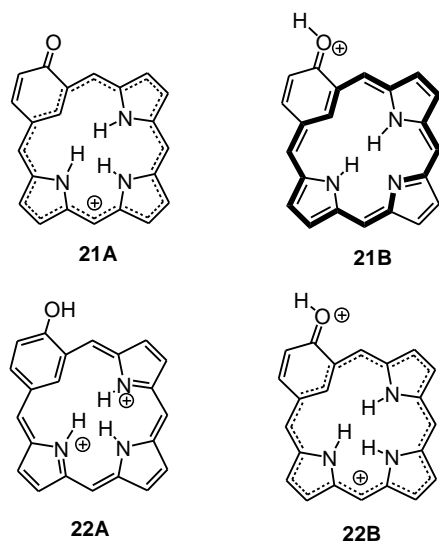
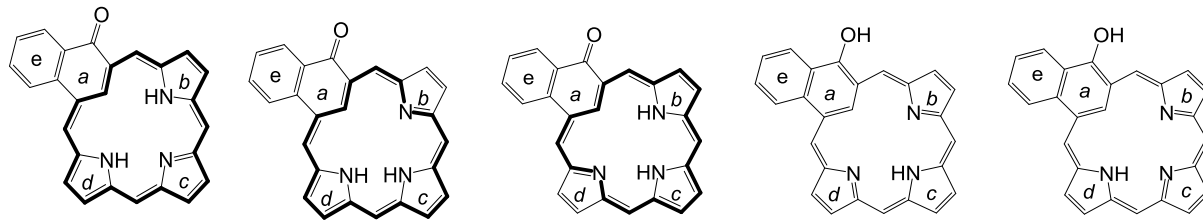


Figure 15. Selected conjugated pathways in protonated oxybenzporphyrins.



	ONP-23,25-H	ONP-23,24-H	ONP-24,25-H	ONP-O,24-H	ONP-O,23-H
Rel. ΔG	0.00	5.12	4.26	19.92	26.71
B3LYP/M06-2X/B3LYP-D	0.00/0.00/0.00	4.64/4.39/4.52	3.95/3.80/3.87	20.09/17.57/20.74	27.29/25.43/28.19
NICS(0)/	-13.32/	-12.90/	-12.88/	-3.91/	-4.16/
NICS(1)zz	-33.41	-32.75	-32.11	-8.18	-9.25
NICS(a)/	+10.22/	+10.70/	+10.82/	-1.94/	-2.19/
NICS(1a)zz	+19.02	+20.01	+16.80	-6.03	-8.42
NICS(b)/	-12.96/	-3.87/	-14.06/	-1.15/	-0.48/
NICS(1b)zz	-32.73	-16.24	-29.74	-8.83	-6.74
NICS(c)/	-3.46/	-12.53/	-12.66/	-6.06/	+0.15/
NICS(1c)zz	-14.05	-28.03	-34.48	-14.89	-6.74
NICS(d)/	-13.31/	-14.51/	-4.35/	-1.71/	-6.44/
NICS(1d)zz	-35.02	-41.54	-16.13	-10.28	-15.21
NICS(e)/	-5.05/	-5.05/	-4.87/	-6.24/	-6.48/
NICS(1e)zz	-17.82	-17.30	-18.39	-21.76	-22.21

Table 13. Calculated energies (hartrees), relative energies (kcal/mol), NICS and NICS_{zz} values (ppm) for tautomers of oxynaphthiporphyrin.

ONP-23,25-H is the favored tautomer for the oxynaphthiporphyrin series (Table 13). Two similar keto tautomers are possible but these are slightly higher in energy due to poorer intramolecular hydrogen bonding interactions. The individual rings in **ONP-23,25-H** are only tilted by 2.72-4.38° relative to the mean macrocyclic plane, although the other two keto forms are slightly more distorted (Table S1). The hydroxy tautomers are much higher in energy (>20° kcal/mol), demonstrating a much larger difference between the keto and hydroxy forms than was seen for oxybenzporphyrin. The bond lengths in **ONP-23,25-H** are consistent with the expected 18 π electron delocalization pathway, and again the 12,13- and 14,15-bonds are relatively long implying greater single bond character. The NICS values for the pyrrole rings are highly aromatic, but the value for pyrrolenine ring *c* is small and ring *a* gives a strongly positive value of +10.22 (Table 13). The ring *c* value of -3.46 may result from dipolar resonance contributors such as **23A** (Figure 16). Ring *a* lies outside of the eighteen-atom delocalization pathway and adjacent to benzene ring *e*, and this leads to the unit being strongly deshielded. The results for keto-forms **ONP-23,24-H** and **ONP-24,25-H** (Table 13) can be analyzed similarly. Hydroxy-tautomers **ONP-O,24-H** and **ONP-O,23-H** are moderately planar and the individual rings are only canted by a few degrees. They also show two minima due to conformations with the OH pointed towards the naphthalene or towards the porphyrinoid ring (Table 14). The energy differences are small, but in these cases the favored conformers have the OH orientated towards the macrocycle. This is due to increased steric interactions resulting from the presence of the naphthalene ring. Tautomer **ONP-O,24-H** gives a NICS(0) value of -3.91, which is consistent with the presence of a weak diatropic ring current. This can be attributed to dipolar canonical forms such as **23B** that possess aromatic delocalization pathways. However, apart from ring *e*, only ring *c* gives a significantly aromatic NICS value and this indicates that a seventeen-atom

18π electron delocalization pathway of the type illustrated in structure **23C** is involved (Figure 16). Similar conclusions can be drawn for tautomer **ONP-O,23-H**, although in this case ring *d* lies within the aromatic pathway. Four tautomers for the monoprotonated form of oxynaphthiporphyrin were considered. In agreement with experimental results, the lowest energy tautomer is the keto form **ONP-23,24,25-H⁺** (Table 15). This structure is somewhat distorted with the individual rings being tilted by 11.05 - 19.62° from the mean macrocyclic plane due in part to the presence of four internal hydrogens. The NICS(0) value is -13.10 , which is consistent with a strongly aromatic species. All of the pyrrole rings give strongly negative values, while ring *a* affords a value of $+11.51$ (Table 15). This indicates that the cationic form favors a nineteen-atom delocalization pathway (structure **24A** in Figure 17). Hydroxy forms **ONP-O,23,25-H⁺**, **ONP-O,23,24-H⁺** and **ONP-O,24,25-H⁺** all gave two conformational minima due to the orientation of the OH (Table 16). Again the differences in energy were small but the favored conformers pointed the OH towards the naphthalene unit, which is the opposite conformation to the favored form for the free base structures. **ONP-O,23,25-H⁺** is the most stable of the hydroxy versions due to the inner hydrogens being optimally arranged for hydrogen bonding interactions, and it gives a significant NICS(0) value of -7.81 (Table 15). The NICS values for pyrrole rings *b* and *d* are strongly aromatic, but rings *a* and *c* give negligible results. These data are consistent with the presence of an 18π electron delocalization pathway as illustrated by structure **24B** (Figure 17). Analysis of the results for the remaining hydroxy-tautomers give rise to similar conclusions. A diprotonated form of oxynaphthiporphyrin is generated at higher acid concentrations. This species is known to have a reduced but still significant diatropic character compared to the free base form. Two conformational minima were noted (Table 17), and the form with the OH orientated towards the naphthalene was shown to be

-2.70 kcal/mol more stable than the conformer with the OH pointed towards the porphyrinoid ring. The diprotonated structure ONP-H_2^{2+} is twisted from planarity due to steric crowding. The NICS(0) value was found to be -8.65, and the reduced aromatic character can be attributed to the availability of resonance contributors such as **25A** (Figure 17). As all three pyrrole rings give strongly aromatic NICS values, while ring *a* gives a low positive value, these results are consistent with the presence of a nineteen-atom 18π electron delocalization pathway as shown for structure **25B** (Figure 17).

ONP-O,24-H-L	ONP-O,24-H-R	ONP-O,23-H-L	ONP-O,23-H-R
-1240.751414	-1240.752706	-1240.739724	-1240.741230
0.81	0.00	0.94	0.00

Table 14. Calculated energies (hartrees) and relative energies (kcal/mol) for hydroxynaphthiporphyrin conformers.

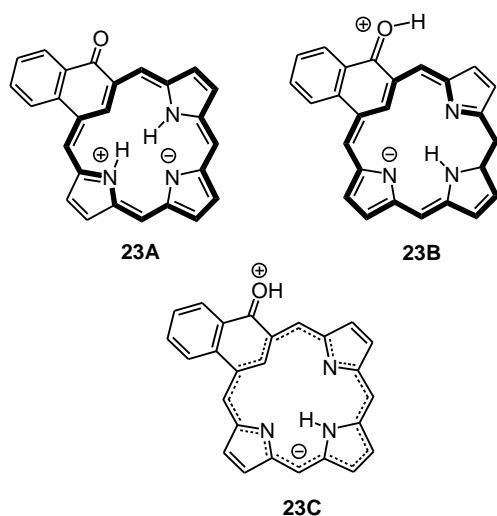
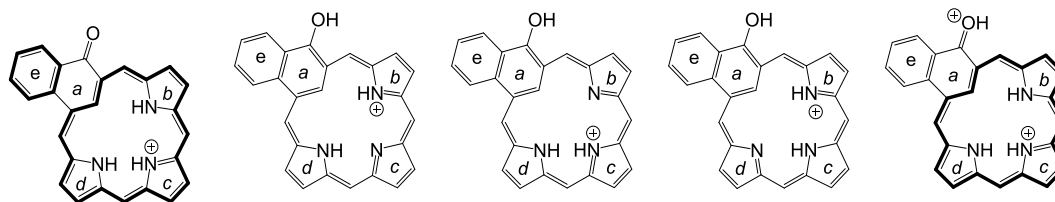


Figure 16. Selected conjugation pathways in oxynaphthiporphyrins.



	ONP-23,24,25-H ⁺	ONP-O,23,25-H ⁺	ONP-O,23,24-H ⁺	ONP-O,24,25-H ⁺	ONPH ₂ ²⁺
Rel. ΔG	0.00	2.82	5.76	5.88	*****
B3LYP/M06-2X/B3LYP-D	0.00/0.00/0.00	3.46/2.86/4.75	6.12/5.09/7.35	6.44/5.64/7.71	*****
NICS(0)/	-13.10/	-7.81/	-7.14/	-6.02/	-8.65/
NICS(1)zz	-31.68	-14.58	-16.37	-13.79	-19.77
NICS(a)/	+11.51/	-1.31/	+0.13/	-0.62/	+1.88/
NICS(1a)zz	+17.31	-4.00	-1.14	-2.53	+3.51
NICS(b)/	-13.93/	-7.97/	-1.62/	-8.39/	-10.33/
NICS(1b)zz	-27.68	-18.10	-9.11	-17.50	-20.60
NICS(c)/	-14.05/	+0.49/	-7.61/	-7.43/	-9.30/
NICS(1c)zz	-45.41	-7.78	-23.73	-21.96	-33.73
NICS(d)/	-14.35/	-8.75/	-9.44/	-2.01/	-10.53/
NICS(1d)zz	-25.26	-19.21	-17.78	-10.02	-18.41
NICS(e)/	-4.86/	-6.38/	-6.08/	-6.17/	-5.37/
NICS(1e)zz	-18.13	-22.64	-21.67	-21.73	-20.12

Table 15. Calculated energies (hartrees), relative energies (kcal/mol), NICS and NICS_{zz} values (ppm) for protonated naphthoporphyrins.

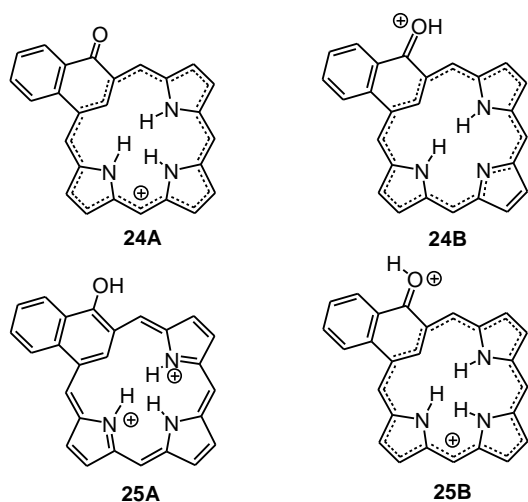


Figure 17. Conjugation pathways in protonated oxynaphthoporphyrins.

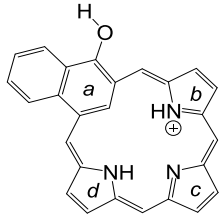
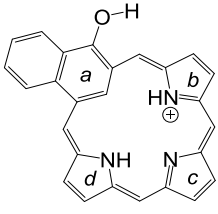
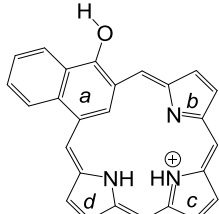
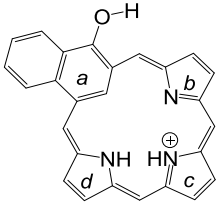
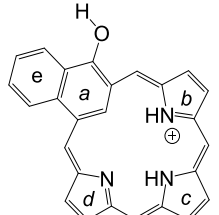
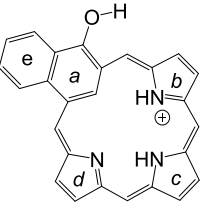
	
ONP-O,23,25-H⁺-L -1241.168371 0.00	ONP-O,23,25-H⁺-R -1241.166710 1.04
	
ONP-O,23,24-H⁺-L -1241.164132 0.00	ONP-O,23,24-H⁺-R -1241.163328 0.50
	
ONP-O,24,25-H⁺-L -1241.163623 0.00	ONP-O,24,25-H⁺-R -1241.161626 1.25

Table 16. Calculated energies (hartrees) and relative energies (kcal/mol) for protonated hydroxynaphthopyrrole conformers.

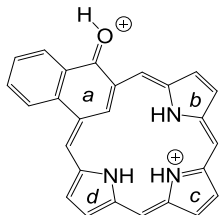
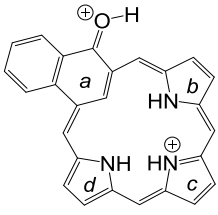
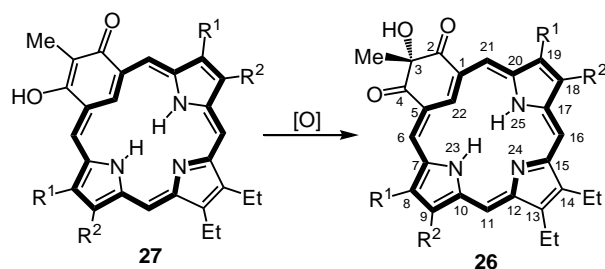
	
ONPH₂²⁺-L -1241.454366 0.00	ONPH₂²⁺-R -1241.450057 2.70

Table 17. Calculated energies (hartrees) and relative energies (kcal/mol) for conformers of diprotonated oxynaphthopyrrole.



Scheme 3. Oxidation of hydroxyoxybenzporphyrins.

Further modified benzporphyrins **26** have also been reported from the oxidation of hydroxyoxybenzporphyrins **27** (Scheme 3).^{52,53} This system is highly diatropic and the internal CH has been observed upfield between -8 and -9 ppm.^{8,53} Two tautomers were considered for this 3-hydroxydioxotetrahydrobenzporphyrin system, **HDBP-23,25-H** and **HDBP-23,24-H** (Table 18). The former tautomer is 3.93-4.05 kcal/mol more stable due to more favorable hydrogen bonding interactions. **HDBP-23,25-H** has bond lengths that are consistent with the presence of an 18 π electron circuit, and the 12,13- and 14,15-carbon-carbon bonds are relatively long indicating that they are not involved in the main delocalization pathway (Figure 18). Both structures are fairly flat, but the six-membered ring is bent due to the presence of a sp³ hybridized carbon atom (Figure 18). However, the aromaticity of the system will only be affected by the three carbon atoms in the six-membered ring that take part in the 18 π electron delocalization pathway. The NICS(0) value for **HDBP-23,25-H** is -14.27. Strongly aromatic values are also obtained for rings *b* and *d*, while the six-membered ring gave a strongly positive result because it lies outside of the 18 π electron delocalization pathway. The pyrroline ring gives a weakly aromatic value of -3.36 and this may be due to resonance contributors such as **28** that introduce alternative delocalization pathways (Figure 18). Similar conclusions can be drawn for **HDBP-23,24-H**. Protonation of this system results in the formation of a highly diatropic

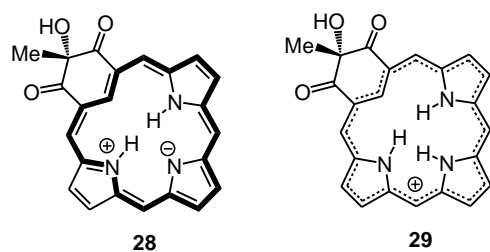


Figure 19. Conjugation pathways in oxidized benziporphyrins.

Conclusion

Benziporphyrins range from nonaromatic species to highly aromatic macrocyclic systems, and as a result they show a remarkable breadth of chemical and spectroscopic properties. Benziporphyrin was assessed using density functional theory and this allowed conformations, bond lengths and relative energies of tautomers to be calculated. Nucleus independent chemical shifts (NICS) and related NICS_{zz} calculations also provided insights into the aromatic character of both the porphyrinoid system as a whole and of the individual component rings. Benziporphyrin has a negligible $\text{NICS}(0)$ value but a degree of diatropicity can be seen upon protonation or the introduction of electron-donating methoxy groups. Tautomerization of 2-hydroxybenziporphyrin is also favored to give an aromatic semiquinone porphyrinoid. Naphthiporphyrins were similarly analyzed and a highly aromatic oxidized benziporphyrin system was also considered. The aromatic delocalization pathways in these systems have been reconsidered and contributing pathways that involve 17, 18, 19 and 20-atom circuits have been identified. The results allow earlier experimental data to be better understood and will facilitate future investigations in this area.

Experimental Section

All calculations were performed using Gaussian 09⁵⁴ Rev D.01 running on a Linux-based PC. Energy minimization and frequency calculations of the porphyrinoid systems were performed at the Density Functional Theory (DFT) level of theory with the B3LYP functional and a 6-311++G(d,p) basis set. Single point energy calculations were performed on the minimized structures using both the B3LYP-D and M062-X functionals and a 6-311++G(d,p) basis set. Mercury 3.1 running on an OS X platform, as provided by the CCDC, www.ccdc.cam.ac.uk/mercury/, was used to visualize the optimized structures. The resulting Cartesian coordinates of the molecules can be found in the electronic supplementary information section. NICS values were computed using the GIAO method,⁵⁵ at the DFT level with the B3LYP functional and a 6-31+G(d,p) basis set, at several positions in each molecule. NICS(0) was calculated at the mean position of all the heavy atoms. NICS(a), NICS(b), NICS(c), NICS(d) and NICS(e) values were obtained by applying the same method to the mean position of the heavy atoms that comprise the individual rings of each macrocycle. In addition, NICS(1)zz, NICS(1a)zz, NICS(1b)zz, NICS(1c)zz, NICS(1d)zz and NICS(1e)zz were obtained by applying the same method to ghost atoms placed 1 Å above each of the corresponding NICS(0) points and extracting the ZZ contribution of the magnetic tensor.

Acknowledgements

This work was supported by the National Science Foundation under grant no. CHE-1212691, and the Petroleum Research Fund, administered by the American Chemical Society.

Electronic supplementary information (ESI) is available.

REFERENCES

1. T. D. Lash, S. T. Chaney and Richter, *J. Org. Chem.*, 1998, **63**, 9076-9088.
2. T. D. Lash, In *Handbook of Porphyrin Science – With Applications to Chemistry, Physics, Material Science, Engineering, Biology and Medicine*, Vol. 16, K. M. Kadish, K. M. Smith and R. Guilard, eds.; World Scientific Publishing: Singapore, 2012, pp 1-329.
3. M. Stepien and L. Latos-Grazynski, *Acc. Chem. Res.*, 2005, **38**, 88-98.
4. M. Stepien and L. Latos-Grazynski, *J. Am. Chem. Soc.*, 2002, **124**, 3838-3839.
5. K. Berlin and E. Breitmaier, *Angew. Chem., Int. Ed. Engl.*, 1994, **33**, 1246-1247.
6. T. D. Lash, *Angew. Chem. Int. Ed. Engl.*, 1995, **34**, 2533-2535.
7. T. D. Lash, A. M. Young, J. M.; Rasmussen and G. M. Ferrence, *J. Org. Chem.*, 2011, **76**, 5636-5651.
8. D. T. Richter and T. D. Lash, *Tetrahedron*, 2001, **57**, 3659-3673.
9. (a) J. T. Szymanski and T. D. Lash, *Tetrahedron Lett.*, 2003, **44**, 8613-8616. (b) T. D. Lash, J. T. Szymanski and G. M. Ferrence, *J. Org. Chem.*, 2007, **72**, 6481-6492.
10. For examples of oxybenzporphyrin-like structures in the phthalocyanine series, see: (a) R. Costa, A. J. Schick, N. B. Paul, W. S. Durfee and C. J. Ziegler, *New J. Chem.*, 2011, **35**, 794-799. (b) A. Muranaka, S. Ohira, D. Hashizume, H. Koshino, F. Kyotani, M. Hirayama and M. Uchiyama, *J. Am. Chem. Soc.*, 2012, **134**, 190-193. (c) N. Toriumi, A. Muranaka, K. Hirano, K. Yoshida, D. Hashizume and M. Uchiyama, *Angew. Chem. Int. Ed.*, 2014, **53**, 7814-7818.
11. J. A. El-Beck and T. D. Lash, *Org. Lett.*, 2006, **8**, 5263-5266.
12. T. D. Lash, J. M. Rasmussen, K. M. Bergman and D. A. Colby, *Org. Lett.* 2004, **6**, 549-552.

13. M. Stepien and L. Latos-Grazynski, *Chem.-Eur. J.*, 2001, **7**, 5113– 5117.
14. T. D. Lash and V. R. Yant, *Tetrahedron*, 2009, **65**, 9527-9535.
15. (a) M. Stepien, L. Latos-Grazynski, L. Szterenber, J. Panek and Z. Latajka, *J. Am. Chem. Soc.*, 2004, **126**, 4566-4580. (b) C.-H. Hung, F.-C. Chang, C.-Y. Lin, K. Rachlewicz, M. Stepien, L. Latos-Grazynski, G.-H. Lee and S.-M. Peng, *Inorg. Chem.*, 2004, **43**, 4118-4120.
16. M. Stepien and L. Latos-Grazynski, *Org. Lett.*, 2003, **5**, 3379-3381.
17. C.-H. Hung, G.-F. Chang, A. Kumar, G.-F. Lin, L.-Y. Luo, W.-M.; Ching and E. W.-G. Diao, *Chem. Commun.*, 2008, 978-980.
18. C. Huang, Y. Li, J. Yang, N. Cheng, H. Liu and Y. Li, *Chem. Commun.*, 2010, **46**, 3161-3163.
19. (a) T. D. Lash, *J. Porphyrins Phthalocyanines*, 2011, **15**, 1093-1115. (b) M. Bröring, *Angew. Chem. Int. Ed.*, 2011, **50**, 2436-2438.
20. A. Ghosh in *The Porphyrin Handbook*, Vol. 7, K. M. Kadish, K. M. Smith and R. Guilard, eds.: Academic Press, San Diego, 2000, pp 1-38.
21. (a) A. Ghosh, T. Wondimagegn, T. and H. J. Nilsen, *J. Phys. Chem. B*, 1998, **102**, 10459-10467. (b) A. Ghosh, *Acc. Chem. Res.*, 1998, **31**, 189-198.
22. (a) H. Furuta, H. Maeda and A. Osuka, *J. Org. Chem.*, 2000, **65**, 4222-4226. (b) H. Furuta, H. Maeda and A. Osuka, *J. Org. Chem.*, 2001, **66**, 8563-8572.
23. (a) D. I. AbuSalim and T. D. Lash, *J. Org. Chem.*, 2013, **78**, 11535-11548. (b) D. I. AbuSalim and T. D. Lash, *Org. Biomol. Chem.*, 2013, **11**, 8306-8323.
24. (a) J. Juselius and D. Sundholm, *J. Org. Chem.*, 2000, **65**, 5233-5237. (b) E. Steiner and P. W. Fowler, *Org. Biomol. Chem.*, 2003, **1**, 1785-1789. (c) E. Steiner and P. W. Fowler, *Org.*

- Biomol. Chem.*, 2004, **2**, 34-37. (d) E. Steiner, A. Soncini and P. W. Fowler, *Org. Biomol. Chem.*, 2005, **3**, 4053-4059. (e) E. Steiner and P. W. Fowler, *Org. Biomol. Chem.*, 2006, **4**, 2473-2476.
25. J.-i. Aihara, *J. Phys. Chem. A*, 2008, **112**, 5305-5311.
26. J.-i. Aihara, E. Kimura and T. M. Krygowski, *Bull. Chem. Soc. Jpn.*, 2008, **81**, 826-835.
27. J.-i. Aihara and M. Makino, *Org. Biomol. Chem.*, 2010, **8**, 261-266.
28. Y. Nakagami, R. Sekine and J.-i. Aihara, *Org. Biomol. Chem.*, 2012, **10**, 5219-5229.
29. J.-i. Aihara, Y. Nakagami, R. Sekine and M. Makino, *J. Phys. Chem. A*, 2012, **116**, 11718-11730.
30. J. I. Wu, I. Fernández and P. v. R. Schleyer, *J. Am. Chem. Soc.*, 2013, **135**, 315-321.
31. P. v. R. Schleyer, C. Maerker, A. Dransfeld, H. Jiao and N. J. R. v. E. Hommes, *J. Am. Chem. Soc.*, 1996, **118**, 6317-6318.
32. M. Alonso, P. Geerlings and F. De Proft, *Phys. Chem. Chem. Phys.*, 2014, **16**, 14396-14407.
33. M. Alonso, P. Geerlings and F. De Proft, *Chem. Eur. J.*, 2013, **19**, 1617-1628.
34. P. R. Schreiner, *Angew. Chem. Int. Ed.*, 2007, **46**, 4217-4219.
35. M. D. Wodrich, C. Corminboeuf and P. v. R. Schleyer, *Org. Lett.*, 2006, **8**, 3631-3634.
36. Y. Zhao and D. G. Truhlar, *Theor. Chem. Accounts*, 2008, **120**, 215-241.
37. S. Grimme, S., *J. Comput. Chem.*, 2004, **25**, 1463-1473.
38. M. Toganoh and H. Furuta, *J. Org. Chem.*, 2013, **78**, 9317-9327.
39. D. I. AbuSalim, G. M. Ferrence and T. D. Lash, *J. Am. Chem. Soc.*, 2014, **136**, 6763-6772.
40. D. Li, D. and T. D. Lash, *J. Org. Chem.*, 2014, **79**, 7112-7121.

41. C. Corminboeuf, T. Heine, G. Seifert, P. v. R. Schleyer and J. Weber, *Phys. Chem. Chem. Phys.*, 2004, **6**, 273-276.
42. H. Fallah-Bagher-Shaidaei, C. S. Wannere, C. Corminboeuf, R. Puchta and P. v. R. Schleyer, *Org. Lett.*, 2006, **8**, 863-866.
43. N. S. Mills and K. B. Llagostera, *J. Org. Chem.*, 2007, **72**, 9163-9169.
44. M. Solà, F. Feixes, J. O. C. Jiménez-Halla, E. Matito and J. Poater, *Symmetry*, 2010, **2**, 1156-1179.
45. T. D. Lash, A. M. Toney, K. M. Castans and G. M. Ferrence, *J. Org. Chem.*, 2013, **78**, 9143-9152.
46. T. D. Lash, *Chem. Eur. J.*, 1996, **2**, 1197-1200.
47. K. Berlin and E. Breitmaier, *Angew. Chem. Int. Ed. Engl.*, 1994, **33**, 219-220. See also: A. M. Young and T. D. Lash, *Org. Biomol. Chem.*, 2013, **11**, 6841-6848.
48. Syntheses of pyriporphyrins were reported subsequently: (a) R. Mysliborski, L. Latos-Grazynski and L. Szterenber, *Eur. J. Org. Chem.*, 2006, 3064-3068. (b) T. D. Lash, K. Pokharel, J. M. Serling, V. R. Yant and G. M. Ferrence, *Org. Lett.*, 2007, **9**, 2863-2866.
49. M. Stepien, L. Latos-Grazynski, T. D. Lash and L. Szterenber, *Inorg. Chem.*, 2001, **40**, 6892-6900.
50. DFT calculations have also been reported for 22-hydroxybenzporphyrin: M. Stepien, L. Latos-Grazynski and L. Szterenber, *J. Org. Chem.*, 2007, **72**, 2259-2270.
51. C. J. Medforth in *The Porphyrin Handbook*; K. M. Kadish, K. M. Smith and R. Guilard, Eds.; Academic Press: San Diego, 2000; Vol. 5, pp 1-80.
52. K. Miyake and T. D. Lash, *Chem. Commun.*, 2004, 178-179.
53. T. D. Lash, K. Miyake, L. Xu and G. M. Ferrence, *J. Org. Chem.*, 2011, **76**, 6295-6308.

54. Gaussian 09, Revision D.01, M. J. Frisch, G. W. Trucks, H. B. Schlegel, G. E. Scuseria, M. A. Robb, J. R. Cheeseman, G. Scalmani, V. Barone, B. Mennucci, G. A. Petersson, H. Nakatsuji, M. Caricato, X. Li, H. P. Hratchian, A. F. Izmaylov, J. Bloino, G. Zheng, J. L. Sonnenberg, M. Hada, M. Ehara, K. Toyota, R. Fukuda, J. Hasegawa, M. Ishida, T. Nakajima, Y. Honda, O. Kitao, H. Nakai, T. Vreven, J. A. Montgomery, Jr., J. E. Peralta, F. Ogliaro, M. Bearpark, J. J. Heyd, E. Brothers, K. N. Kudin, V. N. Staroverov, R. Kobayashi, J. Normand, K. Raghavachari, A. Rendell, J. C. Burant, S. S. Iyengar, J. Tomasi, M. Cossi, N. Rega, N. J. Millam, M. Klene, J. E. Knox, J. B. Cross, V. Bakken, C. Adamo, J. Jaramillo, R. Gomperts, R. E. Stratmann, O. Yazyev, A. J. Austin, R. Cammi, C. Pomelli, J. W. Ochterski, R. L. Martin, K. Morokuma, V. G. Zakrzewski, G. A. Voth, P. Salvador, J. J. Dannenberg, S. Dapprich, A. D. Daniels, Ö. Farkas, J. B. Foresman, J. V. Ortiz, J. Cioslowski and D. J. Fox, Gaussian, Inc., Wallingford CT, 2009.
55. K. Wolinski, J. F. Hinton and P. Pulay, *J. Am. Chem. Soc.*, 1990, **112**, 8251-8260.